Modeling of a High Throughput Hot-Wall Reactor for Selective Epitaxial Growth of Silicon

Carl Galewski, *Member, IEEE,* and William G. Oldham, *Fellow, IEEE*

Abstract—**A tubular hot-wall silicon epitaxial reactor operated in the selective deposition regime is characterized for growth rate uniformity in both the radial and longitudinal directions. The range of experimental conditions includes temperatures from 900°C to 800°C, pressures from 1 torr to 0.4 torr, concentrations of SiH_2Cl_2 in H_2 from 17% to 4%, and wafer diameters from 125 mm to 75 mm. The simplest possible models that accurately predict these data are formulated; in the radial direction a simple first-order model is sufficient, whereas in the longitudinal direction it is necessary to include the entrance region of the reactor and transport by diffusion. The resulting simulator is used to demonstrate improvements to the existing hot-wall reactor, and to propose a design for a scaled up production-sized hot-wall reactor. The hypothetical production-sized reactor accommodates 100 wafers of 200 mm diameter. Predicted throughputs for selective epitaxial silicon layers are 16 wafers/hour for 1 μm thick layers, and 27 wafers/hour for 1700 Å thick layers.**

I. Introduction

MANY element and useful device structures become possible with the availability of selectively deposited epitaxial silicon layers. However, a low-cost approach may be necessary to make them practical solutions for the complex integrated circuits of the future. An example of such a structure is the raised source/drain transistor described by Rodder and Yeakley [1] which requires a 1700 Å thick selectively deposited silicon epitaxial layer. For this application, a tubular hot-wall reactor able to deposit selective epitaxy at a rate of about 100 Å/min on a batch of 100 wafers would provide more accurate thickness control and lower cost than current cold-wall reactors, especially for wafer sizes of 200 mm and above.

Typically, epitaxial deposition of silicon requires high temperatures that are not compatible with hot-wall reactors because of the severe depletion effects that result. We have found experimentally that it is possible with careful consideration of the reactor design, deposition conditions, and wafer cleaning to use low deposition temperatures that reduce depletion effects while still resulting in defect-free epitaxial silicon [2], [3]. Devices fabricated on wafers with these epitaxial layers have been found to be indistinguishable from devices fabricated simultaneously on standard substrates [4].

It is the intent of this article to explore the feasibility of a production-sized hot-wall silicon epitaxy reactor for 200 mm diameter. An experimental reactor has been constructed by modifying a commercial low-pressure chemical vapor deposition (LPCVD) furnace [5], [6]. Growth rate data from this reactor is used to formulate a physical model that predicts the deposition uniformity in both the radial and longitudinal directions. The model is used to propose improvements to the existing reactor, and to propose a design for a system that can accommodate 100 wafers of 200 mm diameter. The throughput of the proposed reactor is found to compare favorably to a typical cold-wall reactor.

II. Modeling of Hot-Wall Tubular Deposition Systems

Low-pressure tubular hot-wall type reactors are presently used to deposit many different materials, providing considerable impetus for improving the understanding and control of such reactors. Physical reactor models for polysilicon [7]–[12], silicon nitride [13], and silicon dioxide from tetraethoxysilane (TEOS) [14] have, for example, been desribed in the literature. None of these studies, however, has included the actual entrance region of the reactor as a part of the model. The models published by Joshi [9] and Yeckel *et al.* [11] include an entrance region, but only as an empty tube of constant temperature. The actual entrance region is quite complicated as shown in the schematic of our system in Fig. 1. Besides a rapidly changing temperature there is also a set of "baffles" that are used to reduce radiant heat losses. These baffles restrict the flow and provide considerable surface area for deposition. Significant errors can arise if the ends of the reactor are ignored by applying ad-hoc boundary conditions at the ends of the region containing the load of wafers. In our model we will extend the simulation far enough toward the ends of the reactor so that boundary conditions of no deposition outside of the region are accurate.

Our objective will be to construct the simplest possible models that explain our data. The physical processes that will be considered are: convection, diffusion, and chemical reaction. As illustrated by the arrows in Fig. 1, reac-

Manuscript received May 30, 1991; revised March 10, 1992. This work was supported by IBM Corporation and the Semiconductor Research Corporation.

The authors are with the Department of Electrical Engineering and Computer Science, University of California at Berkeley, Cory Hall, Berkeley, CA 94720.

IEEE Log Number 9201185.

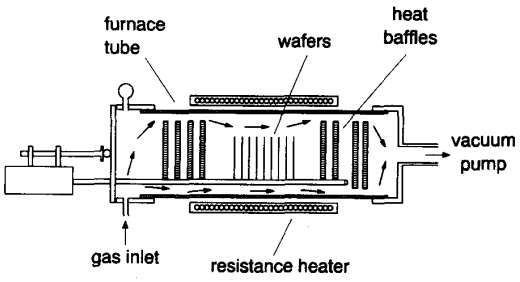

Fig. 1. Schematic of the experimental hot-wall reactor. The arrows illustrate the path of the gas inside the reactor.

tants are transported along the axis of the tube from left to right by convection and diffusion. The reaction that forms solid silicon on the wafers and reactor walls depletes the gas phase of reactants and generates reaction products. Transport by diffusion is a particularly important component of the reactor model because convection cannot efficiently aid the transport of gas to the center of the wafers which are oriented perpendicularly to the main gas flow. In most cases the resulting radial uniformity constraint determines the design and operation of the whole system. For example, reduced pressure operation is often necessary since it simultaneously decreases the deposition rate and increases the diffusion rate.

III. Radial Depletion Model

Yeckel *et al.* [15] have shown that—for the typical LPCVD conditions encountered in a tubular hot-wall system—the dominant transport mechanism between the wafers is diffusion, and that the longitudinal concentration gradient across the wafer space can be ignored. In our model it will be assumed that a uniform concentration in the annular region supplies the gaseous reactant for each wafer, and that the reaction rate is first-order in SiH_2Cl_2. These simplifying assumptions can be justified by noting that our interest is in uniform conditions, implying small concentration variations. It also is assumed that the wafers are placed concentrically within the tube without the use of any cantilevers or "boats" to hold them in place. This is, of course, impossible in reality; however, it was found experimentally that the obstruction provided by the boat and cantilever improves uniformity. This observation agrees with the improvement in radial uniformity described by Yeckel *et al.* [16] with wafer carriers that deliberately reduce the growth rate along the edge. Excluding the effect of the cantilever and boat is, therefore, a worst-case condition.

As shown in Fig. 2, the above assumptions reduce the radial depletion model to a simple one-dimensional mass-balance. In cylindrical coordinates the mass-balance can be written as

$$\delta \frac{d}{dr}\left(rD\frac{dC}{dr}\right) - \alpha r k_s' C = 0 \qquad (1)$$

where δ is the space between the wafers, C is the concentration of SiH_2Cl_2, D is the binary diffusion constant of

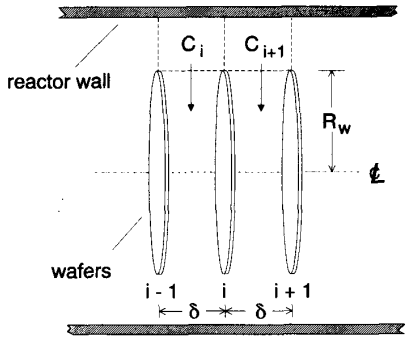

Fig. 2. Radial depletion model resulting from the simplifying assumption that transport occurs by radial diffusion from a uniform annular concentration of reactant.

SiH_2Cl_2 and H_2, k_s' is the surface-rate constant for deposition, and α is the silicon coverage factor. The silicon coverage factor α is equal to the total area of silicon on the two wafers that bound the space divided by the total wafer area. It is included because deposition is selective with respect to SiO_2. If no oxide is present on either of the two wafer surfaces $\alpha = 2$.

The binary diffusion constant D [cm^2/sec] for SiH_2Cl_2 and H_2 can be estimated from Chapman–Enskog kinetic theory [17] according to the following expression

$$D_{AB} = 0.0018583 \frac{\sqrt{T^3\left(\frac{1}{M_A}+\frac{1}{M_B}\right)}}{P\sigma_{AB}^2\Omega_{D,AB}} \qquad (2)$$

It is assumed in (2) that the ideal gas law is valid. The variables are defined as follows: P is the pressure [atm], T is the absolute temperature [°K], M is the respective molecular weights [g/mole], σ is a characteristic diameter of the molecules [Å], and $\Omega_{D,AB}$ is a slowly varying function of the dimensionless temperature kT/ϵ. A more convenient representation for our purposes is given by

$$D_{AB} \approx D_o\left(\frac{P_o}{P}\right)\left(\frac{T}{T_o}\right)^{1.65} \qquad (3)$$

where D_o at temperature T_o and pressure P_o is calculated according to (2). The overall temperature dependence of (2) is approximated by the power 1.65 in the temperatures range of interest [17]. If Lennard–Jones parameters for CH_2Cl_2 are used as an analog to SiH_2Cl_2 in (2) then D_o is 5700 cm^2/sec at the typical operating conditions of 850°C and 0.6 torr.

The first-order deposition rate expression is of the form

$$r_{dep} = k_s P_{DCS} = k_{so} e^{-E_A/kT} P_{DCS} \text{ [cm/sec]} \qquad (4)$$

where P_{DCS} is the SiH_2Cl_2 partial pressure, and k_s is a reaction-rate constant obeying an Arrhenius relationship with activation energy E_A. Conversion of the deposition rate to a flux as a function of concentration is accomplished by defining a new surface-rate constant k_s' as in

$$R_{dep} = k_s' C = k_s m_{Si} RTC \text{ [moles/sec-cm}^2\text{]} \qquad (5)$$

where m_{Si} is the molar density of silicon equal to $8.31 \cdot 10^{-2}$ moles/cm^3, R is the ideal gas constant, T is the absolute temperature, and C is the concentration of SiH_2Cl_2 [moles/cm^3].

The concentration C_i is constant in the annular region of the ith wafer. At the center of each wafer the cylindrical symmetry of the problem forces the gradient to zero. The result is the following boundary conditions for (1):

$$C(R_W) = C_i \tag{6}$$

$$\frac{dC}{dr}(0) = 0 \tag{7}$$

A general solution to (1) can be obtained by defining the following dimensionless parameters:

$$\psi \equiv \frac{C}{C_i} \tag{8}$$

$$\xi \equiv \frac{r}{R_W} \tag{9}$$

$$\phi \equiv R_W \sqrt{\frac{\alpha k_s'}{\delta D}}. \tag{10}$$

The dimensionless factor ϕ is analogous to the Thiele parameter used in chemical engineering. After substituting (8), (9), and (10) into (1) we obtain the following dimensionless differential equation

$$\frac{1}{\xi}\frac{d}{d\xi}\left(\xi \frac{d\psi}{d\xi}\right) - \phi^2\psi = 0 \tag{11}$$

with boundary conditions:

$$\psi(1) = 1 \tag{12}$$

$$\frac{d\psi}{d\xi}(0) = 0. \tag{13}$$

The solution for the normalized concentration ψ defined by (11) is a Bessel function of zero-order and parameter ξ. The normalized concentration at the center, $\psi(\phi, 0)$, can be obtained by a series approximation. Neglecting high-order terms, an expression accurate to 1% for radial depletion up to 20% is given by

$$\psi(\phi, 0) \approx \left(1 + \frac{\phi^2}{4}\right)^{-1} = \left(1 + \frac{R_W^2}{4}\frac{\alpha}{\delta}\frac{k_s'}{D}\right)^{-1}. \tag{14}$$

Thus it is possible to predict the uniformity once the ratio k_s'/D is known. Because of the first-order rate assumption there is no dependence on the concentration of SiH_2Cl_2 in the annular region, making the radial uniformity model independent of longitudinal depletion.

A series of epitaxial silicon depositions were performed on ⟨100⟩ oriented substrates to obtain a model for k_s'/D. The experimental conditions are summarized in Table I. The temperature, pressure, input gas composition, and wafer diameter were varied around a nominally standard set of conditions represented by experiments 177 and 182.

TABLE I
RADIAL UNIFORMITY EXPERIMENTS

Expt. #	Temp. (°C)	Press. (mtorr)	H_2 (sccm)	DCS (sccm)	Wafer dia. (mm)
177	852	620	400	32	100
182	852	622	400	32	100
183	852	622	400	32	75
184	851	621	400	32	125
186	851	393	200	16	100
188	851	1003	800	64	100
191	901	607	400	32	100
192	803	596	400	32	100
193	852	601	312	64	100
194	852	605	452	16	100

Wafers with a 1 μm thick oxide were patterned with narrow concentric oxide circles spaced 4 mm apart in order to maximize depletion and to maintain radial symmetry. The whole-wafer pattern was printed on a transparency and transferred to the wafers by contact photolithography. The wafers were etched in 5 : 1 buffered HF after a 20 sec flood exposure and development. The resulting oxide pattern consisted of 200 μm wide oxide lines, corresponding to 95% silicon coverage independent of wafer size. The wafers were placed in an open boat with slots cut at 2.4 mm intervals so that data for spacings of 2.4, 4.8, 7.2, and 9.6 mm could be obtained. Backs of the wafers were bare, resulting in a worst-case oxide coverage ratio α of 1.95.

Film thicknesses were measured with a stylus profiler after removal of the oxide lines with HF. The uncertainty of the thickness measurements was estimated by measuring a designated reference sample before, and after, each use of the stylus profiler. From this reference sample we obtained a 3σ variation of ±70 Å when averaging the readings from 4 consecutive scans for each measurement. The actual thickness measurements spanned 8,080 Å to 6,090 Å, resulting in an uncertainty between ±1.6% and ±2.2% for normalized data.

Experiment 177 in Table I was an initial exploratory experiment that differed from experiment 182 only in that two sets of variably spaced wafers were used. This experiment demonstrated that the effect of longitudinal depletion was less than the thickness measurement accuracy, validating the choice of a first-order approximation in (4). Raw deposition rate data versus radial position from experiment 177 are shown for the upstream set of wafers in Fig. 3(a). The radial position axis corresponds to a left (negative) to right (positive) diameter as viewed facing the wafer from an upstream position inside the reactor. The left-to-right diameter is well away from the effects caused by the boat and cantilever. It is difficult to discern a trend from the data in the raw form because of the effect of depletion. If, however, the growth rate is normalized to the growth rate at the left (negative) radial position, the influence of spacing and oxide selectivity becomes clearer as illustrated by Fig. 3(b). The normalized growth rate corresponds directly to the normalized concentration ψ because of the first-order reaction-rate assumed in (4).

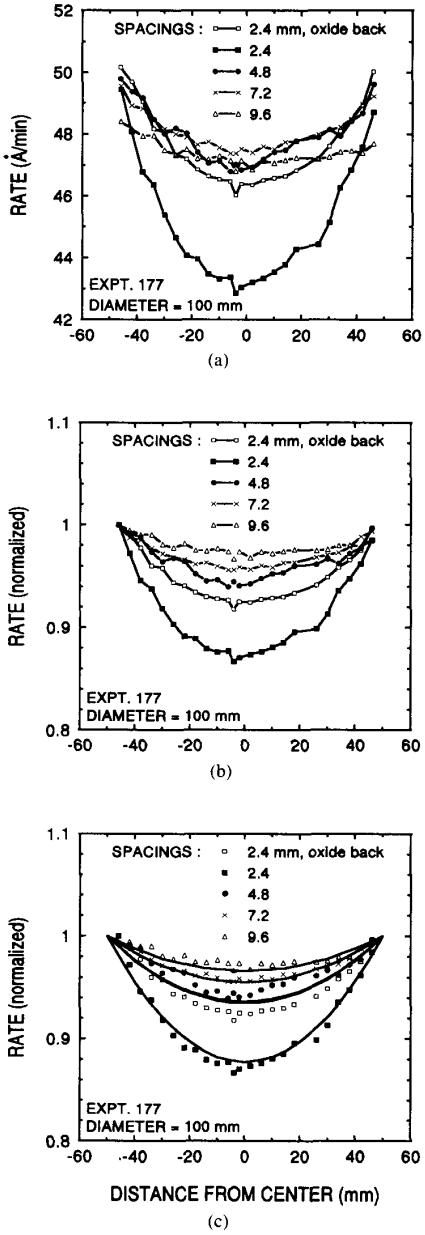

Fig. 3. Radial growth-rate data obtained from the nominally standard conditions represented by experiment 177. Actual deposition rates versus radial position are shown in (a), and data normalized to the growth-rate at the left edge (negative) of each wafer are shown in (b). In (c) the normalized data points are plotted together with the radial model (solid lines).

An expression for k_s'/D was obtained by dividing k_s' as defined by (4) and (5) with the diffusivity D as represented by (3). The result is an equation with two fitting parameters, a constant multiplier and an activation energy. The values of these parameter were obtained by minimizing the sum of square errors between growth-rate data and calculated values for the normalized concentration according to (14). Best fit to the data resulted from the following expression

$$\frac{k_s'}{D} = 1.51 \cdot 10^{11}\left(\frac{P\ (\text{atm})}{[T\ (^\circ\text{K})]^{0.65}}\right) e^{-1.93\,\text{eV}/kT}\ [\text{cm}^{-1}]. \tag{15}$$

The 1.93 eV activation energy of (15) agrees well with the range of activation energies of 1.3 to 2.2 eV that have been reported in the literature for deposition of silicon from SiH_2Cl_2. The final model obtained by substituting (15) into (14) accurately represents the radial variation across the wafers as shown by the solid lines in Fig. 3(c).

For design purposes, the most important aspect is the maximum difference in thickness between the edge and middle of each wafer. In Fig. 4 the normalized rates measured at the centers of the wafers are plotted as points with error bars versus the wafer spacing with wafer diameter, pressure, temperature, and composition as parameters. The values calculated after substitution of (15) into (14) are shown as the solid lines in Fig. 4. The model is within the error bars of the measured data except for a few cases involving the narrowest 2.4 mm spacing. There is some variation in the actual spacing caused by the slots in the boat having to be wider than the wafers they hold. The resulting wafer movements affect the results obtained from the narrowest spacings more than the results from wider ones. Also an important consideration concerning the narrowest spacing is that the mean free path is 0.5 mm at 850°C and 0.6 torr. As a result, the growth rate at the edge may be larger than predicted by (14) for narrow spacings approaching the mean free path.

An effectiveness factor η can be used to incorporate the effect of radial depletion in the longitudinal deposition rate model that will be described in the next section. The formal definition of the effectiveness factor is the ratio of the actual deposition rate across the whole wafer to the rate evaluated using the concentration at the edge of the wafer. The definition of this effectiveness factor is analogous to those used in chemical engineering to relate reaction rates in catalyst pellets to external concentrations. For the linear reaction rate expression defined shown in (5) the expression for the effectiveness factor becomes

$$\eta = \frac{\int_0^{Rw} k_s' C(r) 2\pi r\, dr}{k_s' C(R_W)\pi R_W^2}. \tag{16}$$

Substituting the definition for the normalized variables defined by (8) and (9), and integrating over the low-order terms in the series approximation of the Bessel function that satisfies (11), we obtain the following simple expression

$$\eta = \frac{1 + \frac{\phi^2}{8}}{1 + \frac{\phi^2}{4}}. \tag{17}$$

Because of the first-order reaction rate, the effectiveness

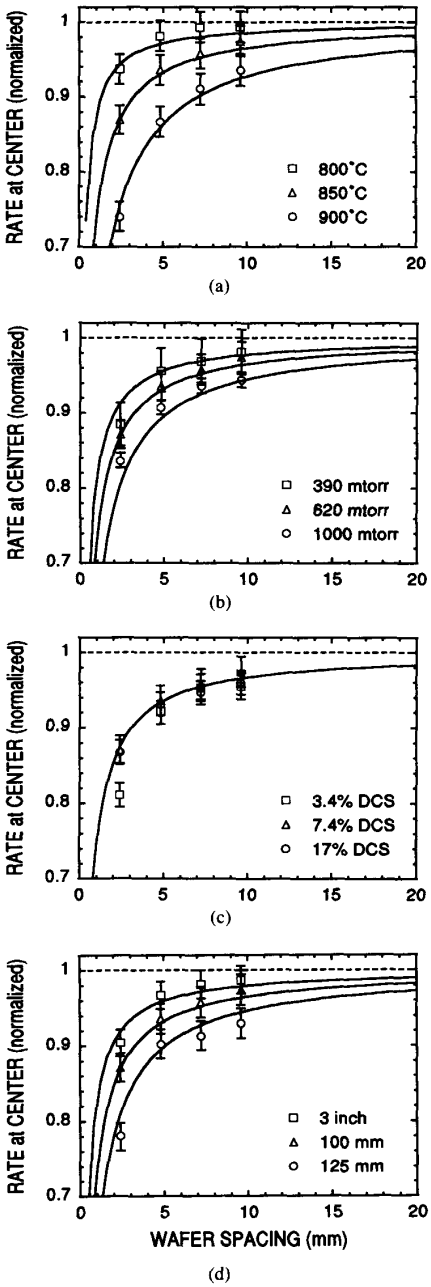

Fig. 4. Comparison between measured data (points) and radial depletion model predictions (solid lines) for experiments that vary: (a) the nominal reactor temperature, (b) the total pressure, (c) the concentration of SiH_2Cl_2 in the input gas stream, and (d) the wafer diameter.

factor in (17) is independent of the variations in reactant concentration along the length of the reactor. The effectiveness factor concept is also valid for more complicated reaction rate expressions, but would no longer be independent of reactant concentrations. In this case, the effectiveness factor would have to be included explicitly in the formulation of the longitudinal model.

IV. Longitudinal Uniformity Model

The non-dimensional Reynolds and Peclet numbers characterize the flow regime in the reactor. The transition from laminar to turbulent flow occurs for Reynolds numbers exceeding 1000, whereas a straightforward evaluation for our reactors predicts values between 1 and 4 [6]. A Reynolds number larger than 0.1 characterizes a transition away from creep flow around objects in the path of the gas. The flow is, therefore, expected to be laminar, but with vortices forming behind edges of objects in the reactor. For simplicity the effect of vortices will not be included.

The Peclet number is a measure of the relative importance of convection versus diffusion. It is defined by

$$\mathrm{Pe} \equiv \frac{uL}{D} \tag{18}$$

in which u is the linear velocity, L a characteristic length, and D the diffusion coefficient. If the Peclet number is much greater than 1, convection dominates. If the Peclet number is much less than 1, diffusion dominates. The same reactor conditions used for the Reynolds number calculation result in Peclet numbers between 1 and 3 [6]. Both convective and diffusive transport must, therefore, be included in the longitudinal model.

Because of the low pressure and high temperature, it will be assumed that radiation is the dominant heat transfer mechanism, and that heat of reaction does not affect the temperature profile. The reactor temperature will, therefore, be radially uniform and equal to the wall temperature. Furthermore, for typical operating conditions, the radial diffusion rate is about 10^3 times larger than the growth rate, leading to the assumption that reactant concentration in the annular region is constant in the radial direction.

Since temperature and reactant concentration vary significantly in the longitudinal direction, a simple first-order reaction-rate expression, such as (4), is not expected to be a good approximation. The thermodynamics of the Si-Cl-H system and the kinetics of silicon deposition from chlorosilanes have been extensively researched, but there is no consensus on a reaction mechanism. The large number of gaseous species that can be formed, and the significant reverse component due to etching by HCl, makes it unlikely that a single reaction mechanism is responsible. Even for a simple heterogeneous reaction, different and quite complex reaction-rate expressions result from assuming that the rate limiting step is: gas phase reaction, adsorption, surface reaction, or desorption [18]. To avoid the ambiguity resulting from postulating a reaction mechanism, an empirical power-law rate-expression describing the overall chemical reaction will be used.

The overall chemical reaction that describes the deposition of silicon in our system can be written as

$$SiH_2Cl_2 \overset{H^2}{\longleftrightarrow} Si_{(s)} + 2\ HCl$$

Hydrogen is not consumed or generated by this reaction

DOCKET ALARM

Explore Litigation Insights

Docket Alarm provides insights to develop a more informed litigation strategy and the peace of mind of knowing you're on top of things.

Real-Time Litigation Alerts

Keep your litigation team up-to-date with **real-time alerts** and advanced team management tools built for the enterprise, all while greatly reducing PACER spend.

Our comprehensive service means we can handle Federal, State, and Administrative courts across the country.

Advanced Docket Research

With over 230 million records, Docket Alarm's cloud-native docket research platform finds what other services can't. Coverage includes Federal, State, plus PTAB, TTAB, ITC and NLRB decisions, all in one place.

Identify arguments that have been successful in the past with full text, pinpoint searching. Link to case law cited within any court document via Fastcase.

Analytics At Your Fingertips

Learn what happened the last time a particular judge, opposing counsel or company faced cases similar to yours.

Advanced out-of-the-box PTAB and TTAB analytics are always at your fingertips.

API

Docket Alarm offers a powerful API (application programming interface) to developers that want to integrate case filings into their apps.

LAW FIRMS
Build custom dashboards for your attorneys and clients with live data direct from the court.

Automate many repetitive legal tasks like conflict checks, document management, and marketing.

FINANCIAL INSTITUTIONS
Litigation and bankruptcy checks for companies and debtors.

E-DISCOVERY AND LEGAL VENDORS
Sync your system to PACER to automate legal marketing.